Cell, Vol. 81, 299–307, April 21, 1995, Copyright © 1995 by Cell Press

A Mechanistic Link between an Inherited and an Acquired Cardiac Arrhythmia: *HERG* Encodes the I_{Kr} Potassium Channel

Michael C. Sanguinetti,*† Changan Jiang,*‡ Mark E. Curran,*‡ and Mark T. Keating*†‡§
*Eccles Program in Human Molecular Biology and Genetics
†Cardiology Division
‡Department of Human Genetics
§Howard Hughes Medical Institute
University of Utah Health Sciences Center
Salt Lake City, Utah 84112

Summary

Mutations in *HERG* cause an inherited cardiac arrhythmia, long QT syndrome (LQT). To define the function of HERG, we expressed the protein in Xenopus oocytes. The biophysical properties of expressed HERG are nearly identical to the rapidly activating delayed rectifier K^+ current (I_{Kr}) in cardiac myocytes. HERG current is K^+ selective, declines with depolarizations above 0 mV, is activated by extracellular K^+, and is blocked by lanthanum. Interestingly, HERG current is not blocked by drugs that specifically block I_{Kr} in cardiac myocytes. These data indicate that HERG proteins form I_{Kr} channels, but that an additional subunit may be required for drug sensitivity. Since block of I_{Kr} is a known mechanism for drug-induced cardiac arrhythmias, the finding that *HERG* encodes I_{Kr} channels provides a mechanistic link between certain forms of inherited and acquired LQT.

Introduction

Long QT syndrome (LQT) causes cardiac arrhythmias and sudden death, often in young, otherwise healthy individuals. LQT can be inherited as an autosomal dominant trait, but the more common form of this disorder is acquired. Many different factors can interact to induce acquired LQT, particularly treatment with certain medications and reduced serum K^+ levels (hypokalemia). Acquired and inherited LQTs are both associated with a distinct arrhythmia known as torsade de pointes. Torsade de pointes is a polymorphic ventricular tachycardia associated with abnormal cardiac repolarization, as detected by QT prolongation on the electrocardiogram, and characterized by sinusoidal twisting of the QRS axis around the isoelectric line (Surawicz, 1989). Torsade de pointes can degenerate into ventricular fibrillation, leading to sudden death.

Recently, we identified mutations in a putative K^+ channel gene, the human *ether-a-go-go*-related gene (*HERG*), in patients with the chromosome 7–linked form of inherited LQT (Curran et al., 1995). *HERG* was initially isolated by Warmke and Ganetzky (1994) by screening a human hippocampal cDNA library with a mouse homolog of *ether-a-go-go*, a Drosophila K^+ channel gene. The function of HERG was unknown, but it was strongly expressed in the heart and was hypothesized to play an important role in repolarization of cardiac action potentials (Curran et al., 1995).

Acquired LQT usually results from therapy with medications that block cardiac K^+ channels (Roden, 1988). The medications most commonly associated with LQT are antiarrhythmic drugs (e.g., quinidine and sotalol) that block the cardiac rapidly activating delayed rectifier K^+ current, I_{Kr}, as part of their spectrum of pharmacologic activity. I_{Kr} has been characterized in isolated cardiac myocytes (Balser et al., 1990; Follmer et al., 1992; Sanguinetti and Jurkiewicz, 1990a; Shibasaki, 1987; Yang et al., 1994) and is known to have an important role in initiating repolarization of action potentials. Despite extensive effort, the gene encoding this channel has not been identified.

To define the physiologic role of HERG, we cloned the full-length cDNA and expressed the channel in Xenopus oocytes. Voltage clamp analyses of the resulting currents revealed that *HERG* encodes a K^+ channel with biophysical characteristics nearly identical to I_{Kr}. These data suggest that *HERG* encodes the major subunit for the I_{Kr} channel and provide a mechanistic link between some forms of inherited and drug-induced LQT.

Results

HERG Encodes a K^+ Channel with Rectification Properties Similar to I_{Kr}

To determine the physiologic properties of HERG, we cloned and characterized a full-length cDNA and prepared it for expression in Xenopus oocytes. The characteristics of the expressed channel were studied in oocytes 2–6 days after cRNA injection using standard two-microelectrode voltage clamp techniques. HERG current was activated in response to test potentials of >-50 mV. The magnitude of HERG current increased progressively with test potentials up to −10 mV (Figure 1A) and then progressively decreased with test potentials of ≥ 0 mV (Figure 1B). Deactivation of current (tail current) was assessed after return of the membrane to the holding potential of −70 mV. The amplitude of the tail currents progressively increased after depolarization and saturated at +10 mV. The HERG current–voltage (I–V) relationship determined for 10 oocytes is shown in Figure 1C. Peak outward current decreased with incremental depolarization, indicating that HERG rectifies. The voltage dependence of channel activation was assessed by plotting the relative amplitude of tail currents as a function of test potential (Figure 1D). HERG reached half-maximal activation at a potential of −15.1 mV. These data define HERG as a delayed rectifier K^+ channel with a voltage dependence of activation and rectification properties nearly identical to I_{Kr} (Sanguinetti and Jurkiewicz, 1990a; Shibasaki, 1987; Yang et al., 1994). These properties are unlike any other known cardiac current.

To characterize HERG further, we determined the time course of current activation and deactivation. The time course for the onset of current (activation) was best fit with a single exponential function (Figure 2A). The rate

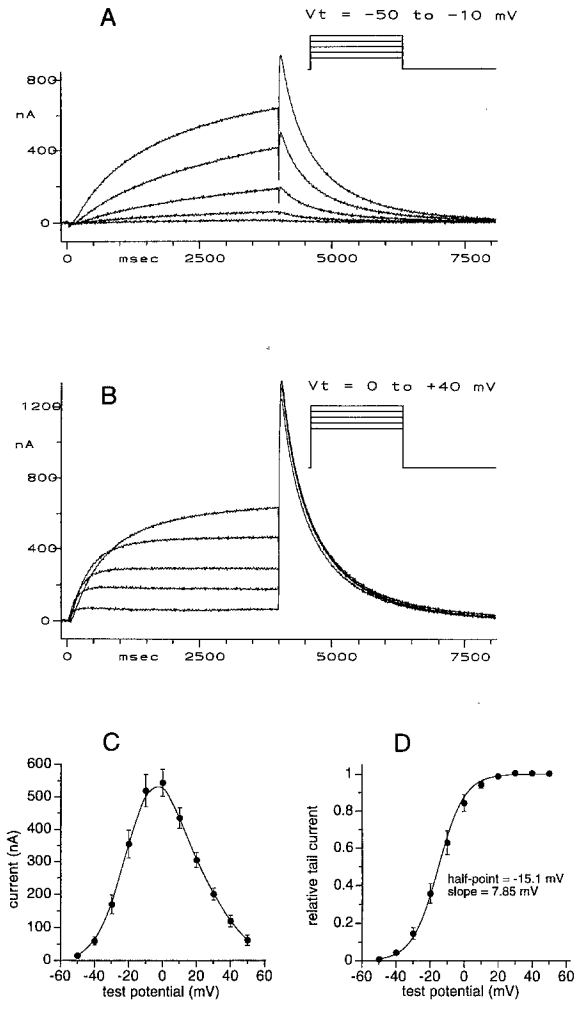

Figure 1. Currents Elicited by Depolarizing Voltage Steps in Xenopus Oocytes Injected with *HERG* cRNA

(A) Currents activated by 4 s pulses, applied in 10 mV increments from −50 to −10 mV. Current during the pulse progressively increased with voltage, as did tail current upon return to the holding potential. Holding potential was −70 mV. The inset illustrates the voltage pulse protocol.

(B) Currents activated with test pulses of 0 to +40 mV, applied in 10 mV increments. Current magnitude during the pulse progressively decreased with voltage, whereas the tail current saturated at +10 mV. Note that currents do not exhibit slow inactivation.

(C) I–V relationship for peak HERG current recorded during 4 s pulses (n = 10).

(D) Voltage dependence of HERG channel activation. Amplitude of tail currents were measured at −70 mV following 4 s pulses and then normalized relative to the largest current. Data were fit to a Boltzmann function:

$$I = 1/(1 + \exp[(V_{½} - V_t)/k]),$$

where I is the relative tail current, $V_{½}$ is the voltage required for half activation of current, V_t is the test potential, and k is the slope factor ($V_{½}$ = −15.1 ± 0.6 mV; k = 7.85 ± 0.2 mV; n = 10).

of activation increased with incremental changes in test potentials from −40 to +50 mV. Deactivating currents were best fit with a biexponential function (Figure 2B), similar to I_{Kr} (Chinn, 1993; Yang et al., 1994). The time constants for HERG current activation and for the fast phase of deactivation were a bell-shaped function of test potential (Figure 2C). The relative amplitude of the fast component of deactivation varied from 0.77 at −30 mV to 0.2 at −120 mV (Figure 2D). The kinetics of HERG current are slower than I_{Kr} (Sanguinetti and Jurkiewicz, 1990a; Shibasaki, 1987; Yang et al., 1994), but exhibit an identical voltage dependence.

HERG Current Is Activated by Extracellular K^+

The K^+ selectivity of HERG was determined by measuring the reversal potential of currents in oocytes bathed in ND96 solution containing different concentrations of KCl (0.5–20 mM). Tail currents were measured at a variable test potential after current activation by a pulse to +20 mV (Figures 3A and 3B). The voltage at which the tail current reversed from an inward to an outward current was defined as the reversal potential, E_{rev}. This varied with extracellular K^+ concentration ($[K^+]_e$), as predicted by the Nernst equation (58 mV change for a 10-fold increase in $[K^+]_e$) for $[K^+]_e$ at ≥5 mM. E_{rev} varied over the entire range of $[K^+]_e$ in a manner well described by the Goldman–Hodgkin–Katz current equation (Figure 3C). These data indicate that HERG is selectively permeable to K^+ over Na^+ by a factor of >100.

A hallmark feature of cardiac I_{Kr} is its modulation by $[K^+]_e$ (Sanguinetti and Jurkiewicz, 1992). The effect of $[K^+]_e$ on the magnitude of HERG current is shown in Figures 4A–4C. HERG current increased in direct proportion to $[K^+]_e$, although the shape of the I–V relationship was not altered (Figure 4D). The $[K^+]_e$ dependence of HERG current was determined by comparing the peak outward current at +20 mV in oocytes bathed in solutions containing 0.5–20 mM KCl. Over this range, HERG current amplitude varied as a linear function of $[K^+]_e$ (Figure 4E). Unlike most other K^+ currents, the magnitude of outward HERG current is paradoxically reduced upon removal of extracellular K^+.

Rectification of HERG Current Results from Rapid Channel Inactivation

Rectification of I_{Kr} is hypothesized to result from voltage-dependent inactivation that is more rapid than activation (Sanguinetti and Jurkiewicz, 1990a; Shibasaki, 1987). The net result of these two competing processes is a reduced current magnitude relative to that predicted from the steady-state activation variable and the electrochemical driving force for outward K^+ flux. It is hypothesized that peak tail currents do not exhibit similar rectification after strong depolarizations (see Figure 1) because the channels recover from fast inactivation much more rapidly than the time course of deactivation. If this interpretation is correct, it should be possible to measure the time course of recovery from fast inactivation during the onset of tail current. Figure 5 shows the results of this experiment. Tail currents were recorded at several test potentials, each preceded by a prepulse to +40 mV (Figure 5A). The voltage dependence of the time constant for recovery from fast inactivation is plotted in Figure 5B. Recovery was slowest at −30 mV (τ = 18.6 ms) and became faster with incremental increases or decreases in test potential. The bell-

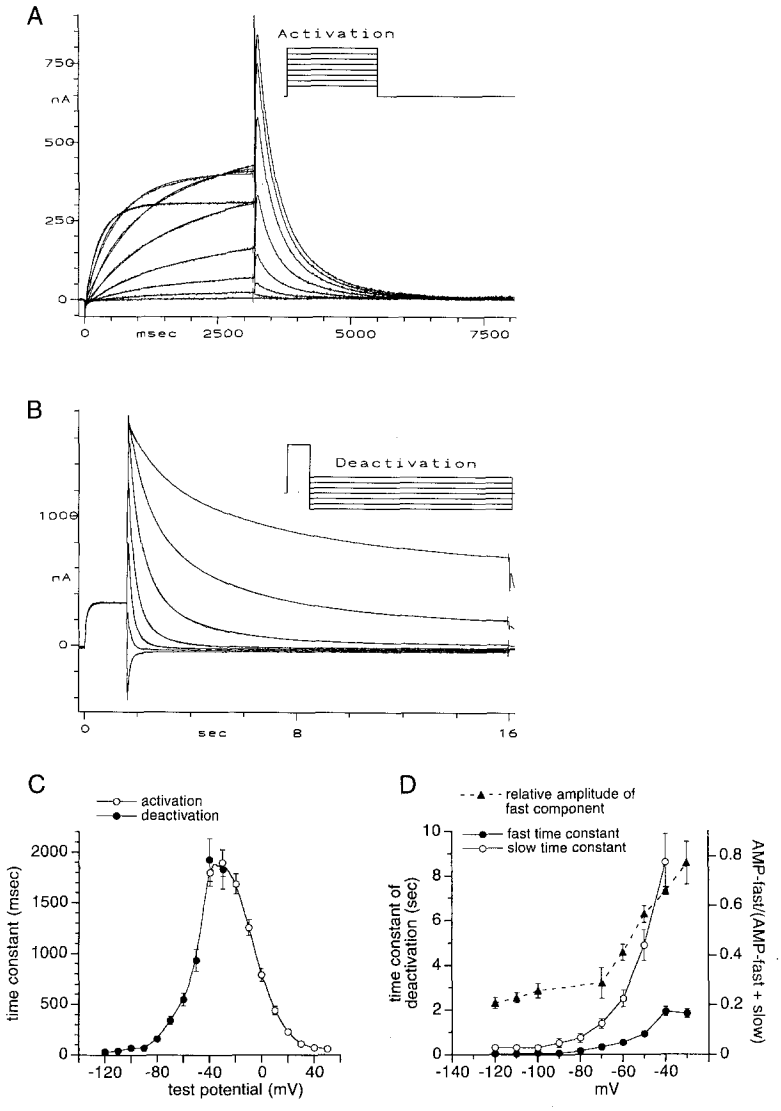

Figure 2. Kinetics of HERG Current Activation and Deactivation

(A) Activating currents were activated by 3.25 s pulses to test potentials ranging from −50 to +20 mV (10 mV steps). Currents and corresponding single exponential fits ($I = A_0 + A_1e^{-t/\tau}$) are superimposed.

(B) Deactivation of HERG currents. Current was activated with 1.6 s pulses to +20 mV, followed by a return to test potentials ranging from −40 to −100 mV (10 mV steps). Deactivating currents and corresponding biexponential fits ($I_{tail} = A_0 + AMP_f \cdot \exp^{-t/\tau f} + AMP_s \cdot \exp^{-t/\tau s}$) are superimposed. Currents were not leak subtracted.

(C) Voltage-dependent kinetics of activation (n = 15) and rapid deactivation (n = 11).

(D) Plot of time constants (τ_f and τ_s) and relative amplitudes of the fast (AMP_f) and slow (AMP_s) components of HERG current deactivation as a function of test potential (n = 11). Relative amplitudes were not determined at −80 and −90 mV owing to the small current magnitudes near the reversal potential.

shaped relationship between the time constant for recovery from inactivation and membrane potential peaked at the same voltage (−30 mV) as the relationship describing the voltage dependence of HERG current activation and deactivation (see Figure 2C). Although the onset of fast inactivation could not be quantified (because it occurred much faster than activation), it is likely that the descending limb of the curve in Figure 5B (from −20 to +20 mV) also describes the voltage dependence of rapid inactivation. These data indicate that rectification of HERG current results from an inactivation process that is much more rapid than the time course of activation.

The voltage dependence of channel rectification was determined by comparison of the fully activated I–V relationship for HERG current (Figure 5C) with the I–V relationship expected for an ohmic conductor. The broken line in Figure 5C was extrapolated from a linear fit of current amplitudes measured at −90 to −120 mV and describes the I–V relationship that would occur in the absence of rectification (ohmic conduction). The slope of this line defines the maximal conductance of HERG in this oocyte (118 μS) and was used to calculate the voltage dependence of channel rectification (Figure 5D). Rectification was half-maximal at −49 mV, and the relationship had a slope factor of 28 mV. The half-point was very similar to I_{Kr} in rabbit nodal cells, and the slope factor was nearly identical to I_{Kr} in guinea pig myocytes (Table 1).

Steady-state HERG current at any given test potential (V_t) can be defined:

$$I_{HERG} = G \cdot n \cdot R \cdot (V_t - E_{rev}),$$

where G is the maximal conductance of HERG current, n is the activation variable, R is the rectification variable, and E_{rev} is the reversal potential.

HERG Current Is Blocked by Lanthanum and Cobalt, but Not Affected by Methanesulfonanilides or Cyclic Nucleotides

I_{Kr} of cardiac myocytes is blocked by 10–100 μM lantha-

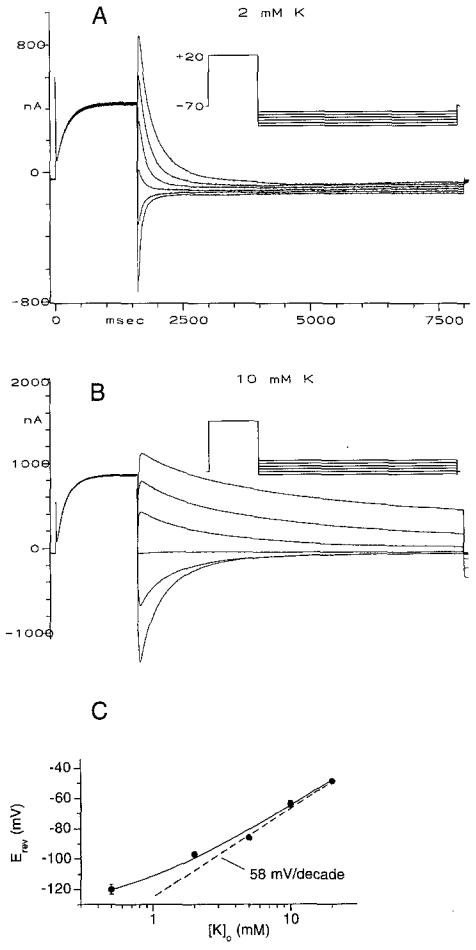

Figure 3. Reversal Potential of HERG Current Varies with $[K^+]_e$, as Expected for a K^+-Selective Channel

(A) Tail currents were elicited at potentials of −105 to −80 mV (applied in 5 mV steps) in an oocyte bathed in ND96 solution ($[K^+]_e$ = 2 mM) following a pulse to +20 mV. The estimated reversal potential of tail currents was −97 mV. Currents were not leak subtracted.

(B) Tail currents were elicited at potentials of −75 to −50 mV (applied in 5 mV steps) in the same oocyte bathed in modified ND96 solution ($[K^+]_e$ = 10 mM). The reversal potential of tail currents was −65 mV.

(C) Reversal potential (E_{rev}) of HERG current varies as a function of $[K^+]_e$. E_{rev} was measured for each oocyte by determining the zero intercept from a plot of tail current amplitude as a function of test potential. Data represent the mean of five determinations, except for 2 mM $[K^+]_e$ (n = 15). The broken line is the relationship predicted by the Nernst equation for a perfectly K^+-selective channel. The solid curve represents a fit of the data to the Goldman–Hodgkin–Katz current equation (Goldman, 1943; Hodgkin and Katz, 1949):

$$E_{rev} = 58 \cdot \log\{(\rho[Na^+]_e + [K^+]_e)/(\rho[Na^+]_i + [K^+]_i)\}.$$

The relative permeability of Na^+ to K^+ (ρ) determined from this fit was 0.007.

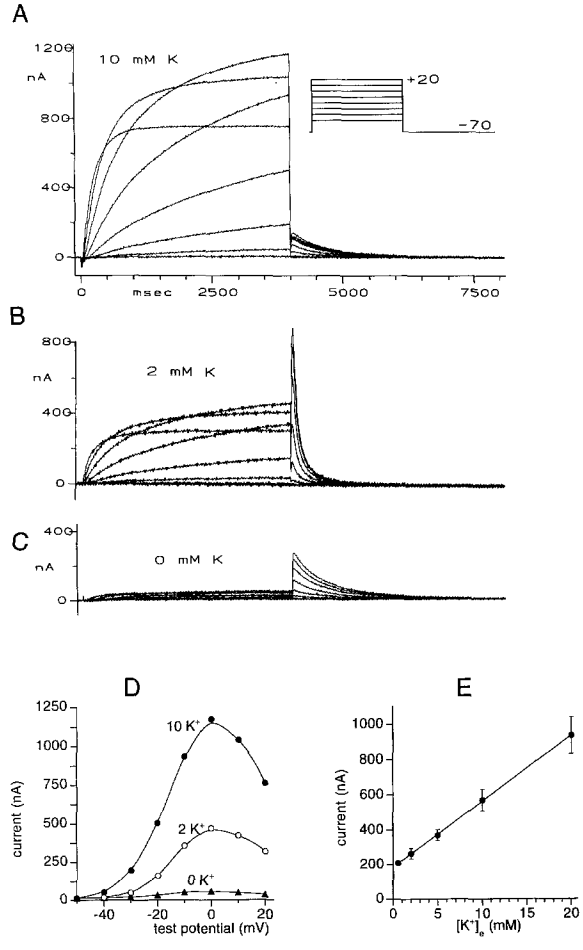

Figure 4. Activation of HERG Current by Extracellular K^+

(A–C) Currents elicited by 4 s pulses to test potentials ranging from −50 to +20 mV in an oocyte bathed in modified ND96 solution containing 10 mM KCl (A) or 2 mM KCl (B) or 5 min after switching to ND96 solution with no added KCl (C).

(D) I–V relationship for currents shown in (A)–(C).

(E) HERG current amplitude varies as a function of $[K^+]_e$. Currents were measured at a test potential of +20 mV (n = 4–6). The solid line is a linear fit to data (I_{HERG} = 189 + 37.5 · $[K^+]_e$). Note that this relationship at lower and higher $[K^+]_e$ would not be expected to be a linear function of $[K^+]_e$.

num (La^{3+}), 2 mM cobalt (Co^{2+}) (Balser et al., 1990; Sanguinetti and Jurkiewicz, 1990b; Sanguinetti and Jurkiewicz, 1991) and by nanomolar concentrations of several methanesulfonanilide antiarrhythmic drugs, such as E-4031 (Sanguinetti and Jurkiewicz, 1990a) and MK-499 (Lynch et al., 1994). We determined whether HERG current is also blocked by these cations and drugs. At a test potential of 0 mV, 10 μM La^{3+} reduced HERG current by 92% ± 3% (n = 4; Figure 6). At least part of the blocking effect of La^{3+} resulted from screening of the negative membrane surface charge (Sanguinetti and Jurkiewicz, 1990b), as indicated by the 40 mV positive shift in both the peak of the I–V relationship (Figure 6C) and the isochronal activation curve (Figure 6D). HERG was also partially blocked (52%) by 2 mM Co^{2+} (n = 2). However, neither E-4031 nor MK-499 at a concentration of 1 μM blocked HERG current, even after the incubation of the oocytes for up to 4 hr in these drugs.

The HERG channel contains a segment homologous to a cyclic nucleotide-binding domain near its carboxyl terminus (Warmke and Ganetzky, 1994). To determine whether HERG was sensitive to cyclic nucleotides, we tested the effect of 8-bromoadenosine 3′,5′-cyclic mono-

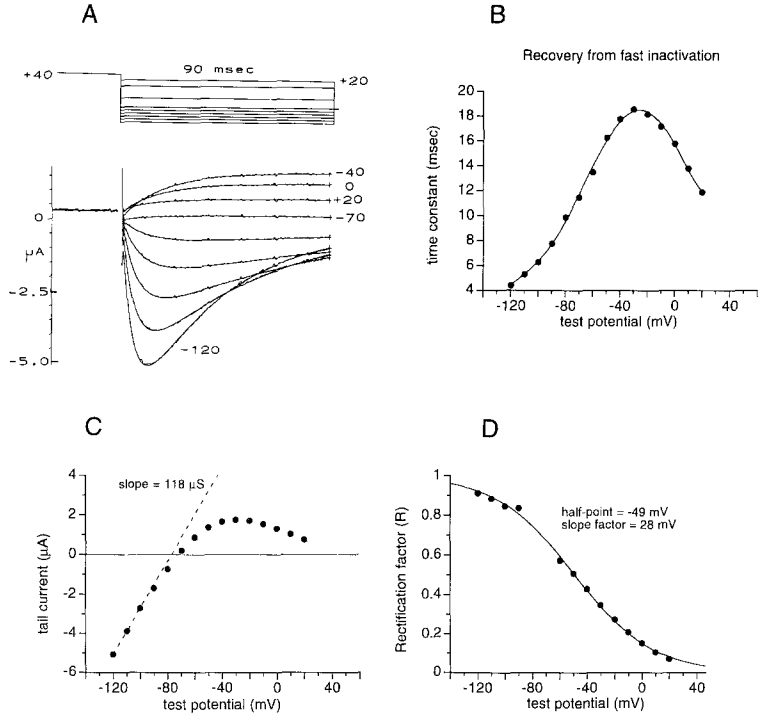

Figure 5. HERG Rectification Results from Rapid Inactivation

(A) Currents recorded at test potentials of +20, 0, −40, and −70 to −120 mV (in 10 mV steps) following activation with a 260 ms pulse to +40 mV ($[K^+]_o$ = 10 mM). Currents were recorded at a sampling rate of 10 kHz. Only the final 30 ms of the activating pulse is shown, followed by the 90 ms tail current. P/3 subtraction was used to eliminate leak current; initial 2 ms of tail currents were blanked. Tail currents recorded at some potentials (+20 to −60 mV) were fit with a single exponential function, since deactivation was slow enough that it did not to contribute significantly to net kinetics of tail current. At more negative potentials (−70 to −120 mV), currents were fit with a biexponential function to account for the fast phase of deactivation that overlapped recovery from inactivation. Fits to the data are superimposed over the current traces.

(B) Time constants for recovery from fast inactivation determined from fits of tail currents as described above.

(C) Fully activated HERG I–V relationship. The maximal conductance of HERG current (118 μS) was determined from the slope of a linear fit to current amplitudes at potentials between −90 and −120 mV.

(D) Voltage dependence of rapid inactivation of HERG current. The rectification factor, R, at each potential was calculated using the current amplitudes plotted in (C): $R = [G \cdot n \cdot (V_t - E_{rev})]/I_{HERG}$, where G is the maximal conductance of HERG (118 μS), n is the activation variable at +40 mV (1.0), V_t is the test potential, and E_{rev} is the reversal potential (−73 mV). The data were fit with a Boltzmann equation: $1/(1 + \exp[(V_t - V_{½})/k])$. The value of $V_{½}$ was −49 mV, and the slope factor (k) was +28 mV.

phosphate (8-Br-cAMP) and 8-bromoguanosine 3′,5′-cyclic monophosphate (8-Br-cGMP) on expressed HERG current. These membrane-permeant analogs of endogenous cyclic nucleotides have been shown to increase the magnitude of other channels expressed in Xenopus oocytes (Blumenthal and Kaczmarek, 1992; Bruggemann et al., 1993). Neither compound had a significant effect on current magnitude or voltage dependence of channel activation at a concentration of 1 mM within 30 min of application (data not shown).

Discussion

HERG Encodes Subunits of Cardiac I_{Kr} Channels

We conclude that *HERG* encodes the major subunit of the cardiac I_{Kr} channel. *HERG* expressed in oocytes induces

Table 1. Comparison of Gating Properties of HERG and I_{Kr}

		I–V Relation		Activation			Inactivation	
Current	Rectification	Peak (mV)	Full Rectification (mV)	Threshold (mV)	Half-Point (mV)	Slope Factor (mV)	Half-Point (mV)	Slope Factor (mV)
HERG[a]	+	0	+60	−50	−15	7.9	−49	+28
I_{Kr} (guinea pig heart)[b]	+	0	+60	−50	−22	7.5	−9	+22
I_{Kr} (rabbit heart)[c]	+	ND	ND	−50	−25	7.4	−68	ND
I_{Kr} (mouse AT-1 cells)[d]	+	10	+55	−50	+1	ND	ND	ND

ND, not determined.

[a] This study.

[b] Jurkiewicz and Sanguinetti, 1993; Lynch et al., 1994; Sanguinetti and Jurkiewicz, 1990a, 1990b; Sanguinetti and Jurkiewicz, 1991.

[c] Carmeliet, 1992; Shibasaki, 1987.

[d] Yang et al., 1994.

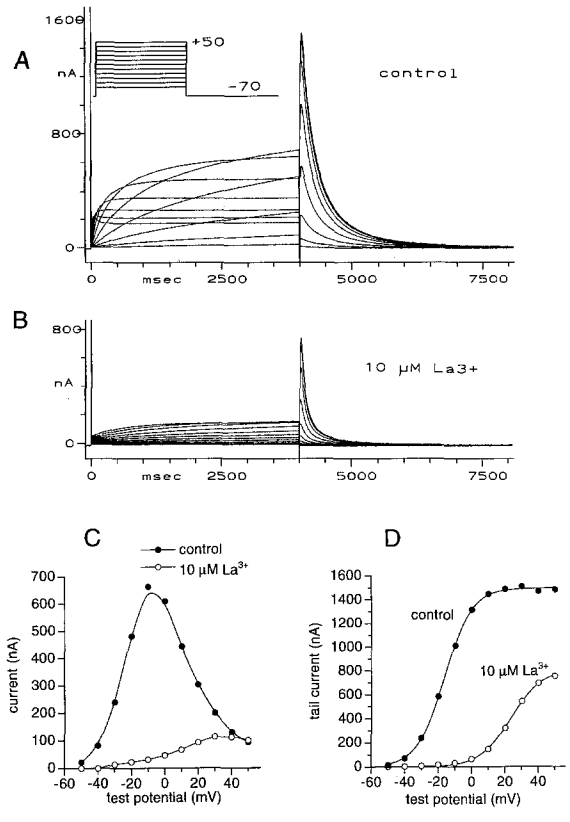

Figure 6. HERG Current Is Blocked by La^{3+}

(A) Control currents activated by 4 s pulses to potentials ranging from −50 to +50 mV. Currents were not leak subtracted.

(B) Currents elicited with the same pulse protocol after exposure of oocyte to 10 μM $LaCl_3$.

(C) I–V relationship of HERG currents measured at the end of 4 s test pulses.

(D) Isochronal activation curves were determined from plots of tail current amplitudes as a funcion of test potential. Data were fitted to a Boltzmann function to obtain the smooth isochronal activation curve. La^{3+} shifted the half-point of activation from −16 mV to +23 mV.

a current that shares most of the distinguishing characteristics defining I_{Kr} in cardiac myocytes (Tables 1 and 2). These include negative slope conductance of the I–V relationship at potentials of >0 mV, with a peak near 0 mV; voltage dependence of activation; paradoxical modulation of current by $[K^+]_e$; and block by La^{3+} and Co^{2+}. The kinetics of activation and deactivation of HERG current are much slower than I_{Kr} in mouse AT-1 cells measured at room temperature (Yang et al., 1994). For example, activation of HERG is about four times slower than I_{Kr} at 0 mV. This difference may indicate that some other endogenous factor or an additional channel subunit modulates the gating of I_{Kr} channels in cardiac cells. In addition, HERG is not activated by 8-Br-cAMP, consistent with the finding that isoproterenol does not increase I_{Kr} in cardiac myocytes (Sanguinetti et al., 1991). Coassembly of HERG subunits in oocytes, presumedly as homotetramers (MacKinnon, 1991), therefore, can reconstitute the major biophysical properties of cardiac I_{Kr}. No other known channel shares all these characteristics. Heterologous expression of HERG will permit future single-channel characterization, a difficult task in cardiac myocytes, where many types of K^+ channels are expressed.

The only major difference between HERG current and I_{Kr} is that HERG is not blocked by methanesulfonanilide drugs (E-4031 and MK-499), potent and specific blockers of I_{Kr} in isolated cardiac myocytes (Lynch et al., 1994; Sanguinetti and Jurkiewicz, 1990a). This suggests that the I_{Kr} channel and the methanesulfonanilide receptor are separate, but interacting, proteins. A similar phenomenon has been described for the K_{ATP} channel, recently isolated from mammalian heart (Ashford et al., 1994). When this channel (rcK_{ATP}-1) is expressed in HEK293 cells, it has all the biophysical characteristics of the native channel (Ashford et al., 1994), including modulation by intracellular nucleotides. However, the channel is not blocked by glibenclamide, a drug that inhibits K_{ATP} channels in cardiac myocytes (Ashford et al., 1994). It may be possible to isolate the methanesulfonanilde receptor biochemically using known high affinity probes such as dofetilide or MK-499. Coexpression of HERG channels with the methanesulfonanilide receptor will enable detailed studies of the interaction between these two molecules.

The Mechanism of HERG Rectification Is Rapid Channel Inactivation

A unique feature of I_{Kr} is negative conductance of the

Table 2. Modulation of HERG and I_{Kr} by $[K^+]_e$ and Blockers

		Blockers			
			Methanesulfonanilides (IC_{50})		
Current	Modulation of Current by $[K^+]_e$	La^{3+} Co^{2+}	E-4031	MK-499	Dofetilide
HERG[a]	+	+	1 μM[b]	1 μM[b]	ND
I_{Kr} (guinea pig)[c]	+	+	397 nM	44 nM	32 nM
I_{Kr} (rabbit)[d]	ND	ND	<0.1 μM	ND	4 nM
I_{Kr} (AT-1 cells)[e]	ND	+	ND	ND	12 nM

ND, not determined.

[a] This study.

[b] No effect.

[c] Jurkiewicz and Sanguinetti, 1993; Lynch et al., 1994; Sanguinetti and Jurkiewicz, 1990a, 1990b; Sanguinetti and Jurkiewicz, 1991.

[d] Carmeliet, 1992; Shibasaki, 1987.

[e] Yang et al., 1994.

I–V relationship at potentials of >0 mV. It has been postulated that rectification of I_{Kr} results from voltage-dependent inactivation that occurs much faster than activation (Shibasaki, 1987). The kinetics of fast inactivation are difficult to resolve in macroscopic current recordings of myocytes and, therefore, were calculated based on kinetics of single-channel activity (Shibasaki, 1987). In this study, we could resolve the time course for recovery from inactivation of macroscopic HERG current because of the large signal-to-noise ratio and the relatively slow channel-gating kinetics at room temperature. The rapid onset of and recovery from fast inactivation explain the negative conductance of the I–V relationship for HERG at potentials of >0 mV. For example, at a test potential of +20 mV, HERG activates with a time constant of 230 ms, but simultaneously inactivates with a time constant of 12 ms. Thus, inactivation is complete before activation of current has reached a significant level, resulting in a much reduced current amplitude. Recovery from inactivation occurs so fast, relative to deactivation, that tail current amplitudes are not significantly affected after repolarization. Our findings support the hypothesis of Shibasaki (1987) that the mechanism of rectification for I_{Kr} (and HERG) is rapid, voltage-dependent inactivation, but does not rule out the possibility that rectification results from block of channels by an endogenous cytoplasmic molecule (Vandenberg, 1987; Fakler et al., 1995).

Rectification of HERG current was half-maximal ($V_{½}$) at −49 mV and had a slope factor of 28 mV. The slope factor of HERG rectification was similar to I_{Kr} measured in guinea pig myocytes (22 mV). The $V_{½}$ of HERG rectification was more negative than that estimated in guinea pig (Table 1). However, the voltage dependence of I_{Kr} rectification in guinea pig myocytes was difficult to measure because of overlap with a much larger I_{K1} at negative test potentials. The absence of overlapping current in rabbit nodal cells and in oocytes expressing HERG allowed more accurate measure of the voltage dependence of channel rectification, and these determinations were similar (Table 1). Single-channel analysis of expressed HERG will enable a more detailed description of voltage-dependent gating and the mechanism of negative conductance of the I–V relationship. This type of analysis is difficult to perform in cardiac myocytes owing to the presence of many types of K^+ channels.

The $[K^+]_e$ Dependence of HERG Current May Modulate Duration of Cardiac Action Potentials

Elevation of $[K^+]_e$ caused an increase in outward HERG current. This is a paradoxical effect, since an increase of $[K^+]_e$ lowers the chemical driving force for outward K^+ flux and therefore would be expected to decrease, rather than increase, outward current. The same phenomenon has been described for I_{Kr} (Sanguinetti and Jurkiewicz, 1992; Scamps and Carmeliet, 1989), but not for any other cardiac channel except I_{K1}. However, I_{K1} is activated almost instantly with hyperpolarization, whereas HERG, like I_{Kr}, is relatively slowly activated by depolarization and is not activated by hyperpolarization.

The modulation of HERG (and I_{Kr}) by $[K^+]_e$ may have physiologic importance. During rapid heart rates or ischemia, K^+ accumulates within intracellular clefts (Gintant et al., 1992). This elevation in $[K^+]_e$ would increase the contribution of HERG (I_{Kr}) to net repolarizing current. HERG (I_{Kr}) may be even more important, therefore, in modulation of action potential duration at high heart rates or during the initial phase of ischemia.

The mechanism of HERG modulation by $[K^+]_e$ is unknown, but the phenomenon has been observed in another cloned K^+ channel, RCK4. The amplitude of RCK4 is also increased with elevation of $[K^+]_e$ (Pardo et al., 1992). Single-channel analyses revealed that elevation of $[K^+]_e$ increased the number of channels available to open, but had no effect on single-channel conductance, mean open time, or gating charge (Pardo et al., 1992). Moreover, it was demonstrated that substitution of a single lysine, located near the pore of the channel, to a tyrosine residue (K533Y) eliminated this effect. A similar $[K^+]_e$-dependent increase in current was created by substitution of a single amino acid near the pore domain of Shaker B channels (Lopez-Barneo et al., 1993). Future experiments will determine whether K^+ modulation of single HERG channels is also affected by a single amino acid mutation.

Mutation of HERG and Drug-Induced Block of I_{Kr}: A Mechanistic Link between Inherited and Acquired LQT

Inherited LQT and the more common (drug-induced) form of the disorder are associated with torsade de pointes, a polymorphic ventricular tachyarrhythmia. We recently showed that mutations in *HERG* cause chromosome 7–linked LQT, likely by a dominant negative inhibition of HERG function (Curran et al., 1995). It should be noted that there are likely to be several different mechanisms that account for acquired and inherited LQT. For example, we recently demonstrated that mutations in *SCN5A*, the cardiac sodium channel gene, cause chromosome 3–linked LQT (Wang et al., 1995). The discovery that *HERG* forms the I_{Kr} channel provides a logical explanation for the observation that block of I_{Kr} by certain drugs can provoke the same arrhythmia (torsades de pointe) as that observed in familial LQT.

Our findings may have important clinical implications. We found that changes in $[K^+]_e$ over a physiologic range significantly modulated the amplitude of HERG current. For example, elevation of $[K^+]_e$ from 2 to 5 mM increased HERG current by 40%. Modest hypokalemia, a common clinical problem, would have a significant effect on HERG current. This may explain the association between hypokalemia and acquired LQT (Roden, 1988). Furthermore, hypokalemia per se has been associated with ventricular arrhythmias (Curry et al., 1976). Medications (e.g., sotalol and dofetilide) that decrease I_{Kr} can be effective antiarrhythmic agents because they modestly lengthen cardiac action potentials, thereby inhibiting reentrant arrhythmias. In the setting of hypokalemia, however, this effect would be exaggerated, leading to excessive action potential prolongation and induction of torsade de pointes. Modest elevation of serum $[K^+]$ in patients given these antiarrhythmic

medications or in individuals with chromosome 7–linked LQT might prevent torsade de pointes.

In summary, we have demonstrated that *HERG* encodes the major subunit forming I_{Kr} channels. This discovery suggests that the molecular mechanism of chromosome 7–linked LQT and certain acquired forms of the disorder can result from dysfunction of the same ion channel.

Experimental Procedures

Cloning of a Full-Length *HERG* cDNA

An *HERG* genomic clone containing domains S1–S3 and intron I (Curran et al., 1995) was used to screen 10^6 recombinants of a human hippocampal cDNA library (Stratagene, library 936205). A single partially processed cDNA clone that contained nucleotides 32–2398 of the *HERG* coding sequence was identified. A second screen of this library was performed using the coding portion of this cDNA. This screen produced a second clone containing *HERG* coding sequence from nucleotides 1216 through the 3′-untranslated region and included a poly(A)$^+$ region. These two cDNAs were ligated using an XhoI site at position 2089. To recover the 5′ region of *HERG*, we screened 10^6 clones of a human heart cDNA library (Stratagene, library 936207) with the composite hippocampal cDNA. A single clone containing the 5′-untranslated region through nucleotide 2133 was isolated. This clone was combined with the hippocampal composite at a BglII site (nucleotide 1913) to produce a full-length *HERG* cDNA.

Construction of an *HERG* Expression Plasmid and Transcription of cRNA

To facilitate *HERG* expression in Xenopus oocytes, the *HERG* cDNA was subcloned into a poly(A)$^+$ expression vector, and the 5′- and 3′-untranslated regions were reduced to minimal lengths. The final *HERG* expression construct contains cDNA sequence from nucleotides −6 through +3513 in the pSP64 plasmid vector (Promega). Before use in expression experiments, the *HERG* construct was characterized by restriction mapping and DNA sequence analyses. Complementary RNAs for injection into oocytes were prepared with the mCAP RNA capping kit (Stratagene) following linearization of the expression construct with EcoRI.

Isolation of Oocytes and Injection of RNA

Xenopus frogs were anesthetized by immersion in 0.2% tricaine for 15–30 min. Ovarian lobes were digested with 2 mg/ml type 1A collagenase (Sigma) in Ca^{2+}-free ND96 solution for 1.5 hr to remove follicle cells. Stage IV and V oocytes (Dumont, 1972) were injected with *HERG* cRNA (0.05 mg/ml; 50 nl) and then cultured in Barth's solution supplemented with 50 μg/ml gentamycin and 1 mM pyruvate at 18°C. Barth's solution contained 88 mM NaCl, 1 mM KCl, 0.4 mM $CaCl_2$, 0.33 mM $Ca(NO_3)_2$, 1 mM $MgSO_4$, 2.4 mM $NaHCO_3$, 10 mM HEPES (pH 7.4).

Two-Microelectrode Voltage Clamp of Oocytes

Unless indicated, oocytes were bathed in ND96 solution. This solution contained 96 mM NaCl, 2 mM KCl, 1 mM $MgCl_2$, 1.8 mM $CaCl_2$, 5 mM HEPES (pH 7.6). In some experiments, KCl was varied by equimolar substitution with NaCl. Currents were recorded at room temperature (21°C–23°C) using standard two-microelectrode voltage clamp techniques. Glass microelectrodes were filled with 3 M KCl and their tips broken to obtain tip resistances of 1–3 MΩ for the voltage-recording electrode and 0.6–1 MΩ for the current-passing electrode. Oocytes were voltage clamped with a Dagan TEV-200 amplifier. Voltage commands were generated using pCLAMP software (version 6; Axon Instruments), a 486DX2 personal computer, and a TL-1 D/A interface (Axon Instruments). Current signals were digitally sampled at a rate equal to two to four times the low pass cutoff frequency (−3 db) of a 4-pole Bessel filter. Unless indicated, currents were corrected for leak and capacitance using standard online P/3 leak subtraction. The oocyte membrane potential was held at −70 mV between test pulses, applied at a rate of 1–3 pulses/min. Data analyses, including exponential fitting of current traces, were performed using pCLAMP. Fits of appropriate data to a Boltzmann function or to a Goldman–Hodgkin–Katz constant field equation (Goldman, 1943; Hodgkin and Katz, 1949) were performed using Kaleidagraph (Synergy Software). Data are expressed as the mean ± SEM (n = number of oocytes).

Acknowledgments

The authors appreciate discussions with J. Mason, W. Barry, L. Ptacek, A. Thorburn, H. Katchuk, and E. Lemaire. This work was supported by National Institutes of Health grants P50-HL 52338-01 and R01-HL48074 and by a Grant-in-Aid from the American Heart Association. E-4031 was a gift from Eisai Tsukuba Research Laboratories. MK-499 was a gift from Merck Research Laboratories.

Received March 30, 1995; revised April 6, 1995.

References

Ashford, M. L. J., Bond, C. T., Blair, T. A., and Adelman, J. P. (1994). Cloning and functional expression of a rat heart K_{ATP} channel. Nature *370*, 456–459.

Balser, J. R., Bennett, P. B., and Roden, D. M. (1990). Time-dependent outward current in guinea pig ventricular myocytes: gating kinetics of the delayed rectifier. J. Gen. Physiol. *96*, 835–863.

Blumenthal, E. M., and Kaczmarek, L. K. (1992). Modulation by cAMP of a slowly activating potassium channel expressed in *Xenopus* oocytes. J. Neurosci. *12*, 290–296.

Bruggemann, A., Pardo, L. A., Stuhmer, W., and Pongs, O. (1993). *Ether-a-go-go* encodes a voltage-gated channel permeable to K^+ and Ca^{2+} and modulated by cAMP. Nature *365*, 445–448.

Carmeliet, E. (1992). Voltage- and time-dependent block of the delayed rectifier K^+ current in cardiac myocytes by dofetilide. J. Pharmacol. Exp. Therap. *262*, 809–817.

Chinn, K. (1993). Two delayed rectifiers in guinea pig ventricular myocytes distinguished by tail current kinetics. J. Pharmacol. Exp. Therap. *264*, 553–560.

Curran, M. E., Splawski, I., Timothy, K. W., Vincent, G. M., Green, E. D., and Keating, M. T. (1995). A molecular basis for cardiac arrhythmia: *HERG* mutations cause long QT syndrome. Cell *80*, 795–804.

Curry, P., Fitchett, D., Stubbs, W., and Krikler, D. (1976). Ventricular arrhythmias and hypokalemia. Lancet *2*, 231–233.

Dumont, J. N. (1972). Oogenesis in *Xenopus laevis* (Daudin). J. Morphol. *136*, 153–180.

Fakler, B., Brandle, U., Glowatzki, E., Weidemann, S., Zenner, H.-P., and Ruppersberg, J. P. (1995). Strong voltage-dependent inward rectification of inward rectifier K^+ channels is caused by intracellular spermine. Cell *80*, 149–154.

Follmer, C. H., Lodge, N. J., Cullinan, C. A., and Colatsky, T. J. (1992). Modulation of the delayed rectifier, I_K, by cadmium in cat ventricular myocytes. Am. J. Physiol. *262*, C75–C83.

Gintant, G. A., Cohen, I. S., Datyner, N. B., and Kline, R. P. (1992). Time-dependent outward currents in the heart. In The Heart and Cardiovascular System, H. A. Fozzard, R. B. Jennings, E. Haber, A. M. Katz, and H. E. Morgan, eds. (New York: Raven Press), pp. 1121–1169.

Goldman, D. E. (1943). Potential, impedance, and rectification in membranes. J. Gen. Physiol. *27*, 37–60.

Hodgkin, A. L., and Katz, B. (1949). The effects of sodium on the electrical activity of the giant axon of the squid. J. Physiol. *108*, 37–77.

Jurkiewicz, N. K., and Sanguinetti, M. C. (1993). Rate-dependent prolongation of cardiac action potentials by a methanesulfonanilide class III antiarrhythmic agent: specific block of rapidly activating delayed rectifier K^+ current by dofetilide. Circ. Res. *72*, 75–83.

Lopez-Barneo, J., Hoshi, T., Heinemann, S. H., and Aldrich, R. W. (1993). Effects of external cations and mutations in the pore region on C-type inactivation of *Shaker* potassium channels. Recept. Channels *1*, 61–71.

Lynch, J. J., Wallace, A. A., Stupienski, R. F., Baskin, E. P., Beare, C. M., Appleby, S. D., Salata, J. J., Jurkiewicz, N. K., Sanguinetti, M. C., Stein, R. B., et al. (1994). Cardiac electrophysiologic and antiar-

rhythmic actions of two long-acting spirobenzopyran piperidine class III agents, L-702,958 and L-706,000 [MK-499]. J. Pharmacol. Exp. Therap. *269*, 541–554.

MacKinnon, R. (1991). Determination of the subunit stoichiometry of a voltage-activated potassium channel. Nature *350*, 232–235.

Pardo, L. A., Heinemann, S. H., Terlau, H., Ludewig, U., Lorra, C., Pongs, O., and Stuhmer, W. (1992). Extracellular K^+ specifically modulates a rat brain K^+ channel. Proc. Natl. Acad. Sci. USA *89*, 2466–2470.

Rosen, D. M. (1988). Arrhythmogenic potential of class III antiarrhythmic agents: comparison with class I agents. In Control of Cardiac Arrhythmias by Lengthening Repolarization, B. N. Singh, ed. (Mount Kisco, New York: Futura Publishing Company), pp. 559–576.

Sanguinetti, M. C., and Jurkiewicz, N. K. (1990a). Two components of delayed rectifier K^+ current: differential sensitivity to block by class III antiarrhythmic agents. J. Gen. Physiol. *96*, 195–215.

Sanguinetti, M. C., and Jurkiewicz, N. K. (1990b). Lanthanum blocks a specific component of I_K and screens membrane surface charge in cardiac cells. Am. J. Physiol. *259*, H1881–H1889.

Sanguinetti, M. C., and Jurkiewicz, N. K. (1991). I_K is comprised of two components in guinea pig atrial cells. Am. J. Physiol. *260*, H393–H399.

Sanguinetti, M. C., and Jurkiewicz, N. K. (1992). Role of external Ca^{2+} and K^+ in gating of cardiac delayed rectifier K^+ currents. Pflügers Arch. *420*, 180–186.

Sanguinetti, M. C., Jurkiewicz, N. K., Scott, A., and Siegl, P. K. S. (1991). Isoproterenol antagonizes prolongation of refractory period by the class III antiarrhythmic agent, E-4031, in guinea pig myocytes: mechanism of action. Circ. Res. *68*, 77–84.

Scamps, F., and Carmeliet, E. (1989). Delayed K^+ current and external K^+ in single cardiac Purkinje cells. Am. J. Physiol. *257*, C1086–C1092.

Shibasaki, T. (1987). Conductance and kinetics of delayed rectifier potassium channels in nodal cells of the rabbit heart. J. Physiol. *387*, 227–250.

Surawicz, B. (1989). Electrophysiologic substrate of *torsade de pointes*: dispersion of repolarization or early afterdepolarizations? J. Am. Coll. Cardiol. *14*, 172–184.

Vandenberg, C. A. (1987). Inward rectification of a potassium channel in cardiac ventricular cells depends on internal magnesium ions. Proc. Natl. Acad. Sci. USA *84*, 2560–2564.

Wang, Q., Shen, J., Splawski, I., Atkinson, D., Li, Z., Robinson, J. L., Moss, A. J., Towbin, J. A., and Keating, M. T. (1995). *SCN5A* mutations associated with an inherited cardiac arrhythmia, long QT syndrome. Cell *80*, 805–811.

Warmke, J. W., and Ganetzky, B. (1994). A family of potassium channel genes related to *eag* in *Drosophila* and mammals. Proc. Natl. Acad. Sci. USA *91*, 3438–3442.

Yang, T., Wathen, M. S., Felipe, A., Tamkun, M. M., Snyders, D. J., and Roden, D. M. (1994). K^+ currents and K^+ channel mRNA in cultured atrial cardiac myocytes (AT-1 cells). Circ. Res. *75*, 870–878.